

Lab Goal:

Analyze the data collected by VectorNAV-100 IMU, and understand the noise characteristics and error distribution in the IMU sensor. Additionally, we are trying to understand the sources of error affecting the sensor.

Methods:

Our team collected 5hrs of data for a stationary imu(fixed using electrical tape) in the basement of Forsyth Hall to model the sensor's noise characteristic. Our selection of time duration for data collection is based on the assumption that 5hr data would be sufficient for estimating all the noise characteristics in our sensor. Further, we collected an additional 5 min data for a stationary sensor to do error analysis. Our study was limited in terms of the sensor's temperature and vibration control environment and computation resources-restricting data collection frequency to 40Hz.

Data Analysis:

5 HOURS STATIONARY DATA

5hr stationary data is used to analyze the noise characteristics of the Gyroscope and Accelerometer sensor, and for this, we are using the Allan Deviation method. This method is commonly used to estimate stability due to sensor noise processes and not for systematic errors. However, this method is limited to characterizing noises for a smaller sampling range, as the probability of correctly estimating noise errors reduces with increasing average sampling size (represented by equation 1) [1]. In our study, we used this method as it captures the required sampling ranges with a probability sufficient for common IMU applications.

$$\sigma(\delta) = \frac{1}{\sqrt{2(\frac{N}{n}-1)}}$$

Equation 1: $\sigma(\delta)$ is the percentage error in estimating $\sigma(\tau)$, n is the total sample, and N is the sampling range (cluster size).

In our analysis, we identified an error in the collected data, which led to an error in estimating in-bias instability for the x-axis in Gyroscope. This error might be due to the effects of temperature or other vibrational effects in the room where data is collected.

Plot 1: Allan deviations (rad/sec) for Gyroscope (Y-Axis) are plotted along with estimated Angle Random Walk (N), Bias Instability(B), and Rate Random Walk(K).

Plot 2: Allan deviation for Modeled and Measured Gyroscope are plotted for comparison. In this plot, we used only the Y axis to model the simulated IMU object, as all the noise parameters were available only for this axis.

Plot 3: Allan deviations (m/sec²) for the x, y, and z axis are plotted along with estimated Angle Random Walk and In-bias stability for the Accelerometer in Plot 3. Additionally, it shows the calculated values of Noise Density equivalent to Angle Random Walk and In-run Bias Stability equivalent to bias instability.

Plot 4: Allan deviations (rad/sec) for the x, y, and z axis are plotted along with estimated Angle Random Walk and In-bias stability for the Gyroscope in Plot 4. Additionally, it shows the calculated values of Noise Density equivalent to Angle Random Walk and In-run Bias Stability equivalent to bias instability.

5 MINUTES STATIONARY DATA

5min stationary data is used to analyze the errors of the Gyroscope, Accelerometer, and Magnetometer along with the estimated Orientation of the sensor by the VectorNAV in-built processing system. We use

Time-series and Frequency Distribution plots to get insight into the measurement trends and the output Error Distribution. For frequency distribution, data points are placed within six bins to represent frequency distribution of errors across mean and standard deviation- [mean-3Std, mean-2Std, mean-Std, mean, mean+Std, mean+2Std, mean+3Std]

Plot 5: Time-series graphs for angular velocity (deg/sec) in the x, y, and z axis are plotted for the Gyroscope along with frequency distribution of data around mean and standard deviation

Plot 6: Time-series graphs for linear acceleration (m/sec²) in the x, y, and z axis are plotted for the Accelerometer along with frequency distribution of data around mean and standard deviation

Plot 7: Time-series graphs for magnetic field (Gauss) in the x, y, and z axis are plotted for the Gyroscope along with frequency distribution of data around mean and standard deviation

Plot 8: Time-series graphs for Euler angles (deg) along the x, y, and z axis are plotted for the Gyroscope along with frequency distribution of data around mean and standard deviation

Results:

Allan Deviation plot allowed us to estimate the White, Pink, and Red Noise characteristics in the IMU unit along with their magnitudes. The estimated noise values are used to simulate an IMU object that shows an Allan Deviation similar to VectorNAV-100. Additionally, these estimated values for Noise Density and in-run bias stability compare well to the performance benchmarks in the Inertial Sensor (VN-100) datasheet. In our comparison, in-run bias stability for Gyroscope should not be compared as the collected data for 5 hr failed to capture this noise characteristic with reliability - observed minima may be local minima, not global minima that capture flicker noise characteristics. Estimated noise values:

	Measured	Datasheet
<i>Gyroscope</i>		
Noise Density ($^{\circ}/s/\sqrt{Hz}$)	0.0060	0.0035
In-run Bias Stability ($^{\circ}/s$)	0.4	3-5
<i>Accelerometer</i>		
Noise Density (mg/ \sqrt{Hz})	0.25	0.14
In-run Bias Stability (mg)	0.04	0.04

In stationary data for 5 min, the gyroscope and accelerometer frequency distribution represents the gaussian distribution, while the magnetic field does not accurately follow the Gaussian distribution. The orientation time-series plot shows an increasing trend as expected from an Extended Kalman Filter processed value. Estimated mean and standard deviation values:

	Mean	Standard Deviation
<i>Gyroscope (deg/sec)</i>		
X-axis	-0.0014	0.0474
Y-axis	-0.0041	0.0490
Z-axis	-0.0100	0.0265
<i>Accelerometer (m/sec²)</i>		
X-axis	0.0764	0.0173
Y-axis	-0.2738	0.0131
Z-axis	-9.5226	0.0223

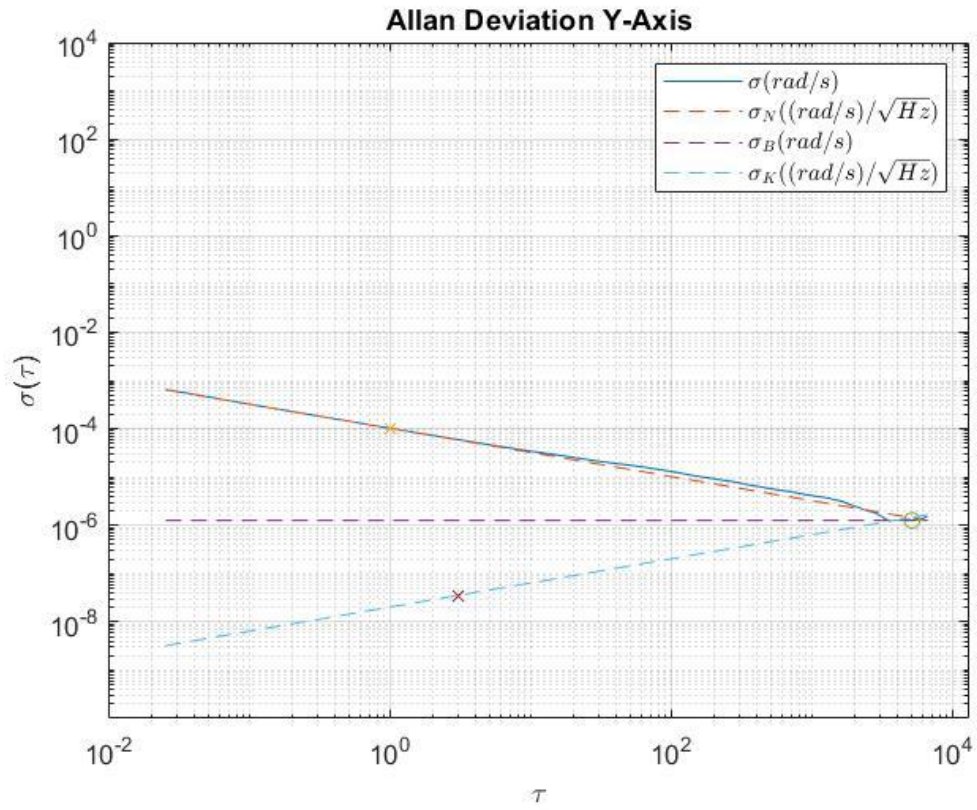
Discussion:

Allan-variance methods allowed the estimation of different Noise-characteristics (white, pink, and red noise) and their magnitudes in the output data of inertial sensors. Our analysis for 5 hr data suggests the leading source of error in the accelerometer output data (up to 100 secs sampling range) and Gyroscope (up to 1000 secs sampling range) is due to Angle Random Walk, which has characteristics of Gaussian white noise. These results are further verified by the 5 min ($\sim 10^2$ secs scale sampling range) stationary data for the accelerometer and Gyroscope. The frequency distribution plot for measurements represents a close reference to the Gaussian distribution.

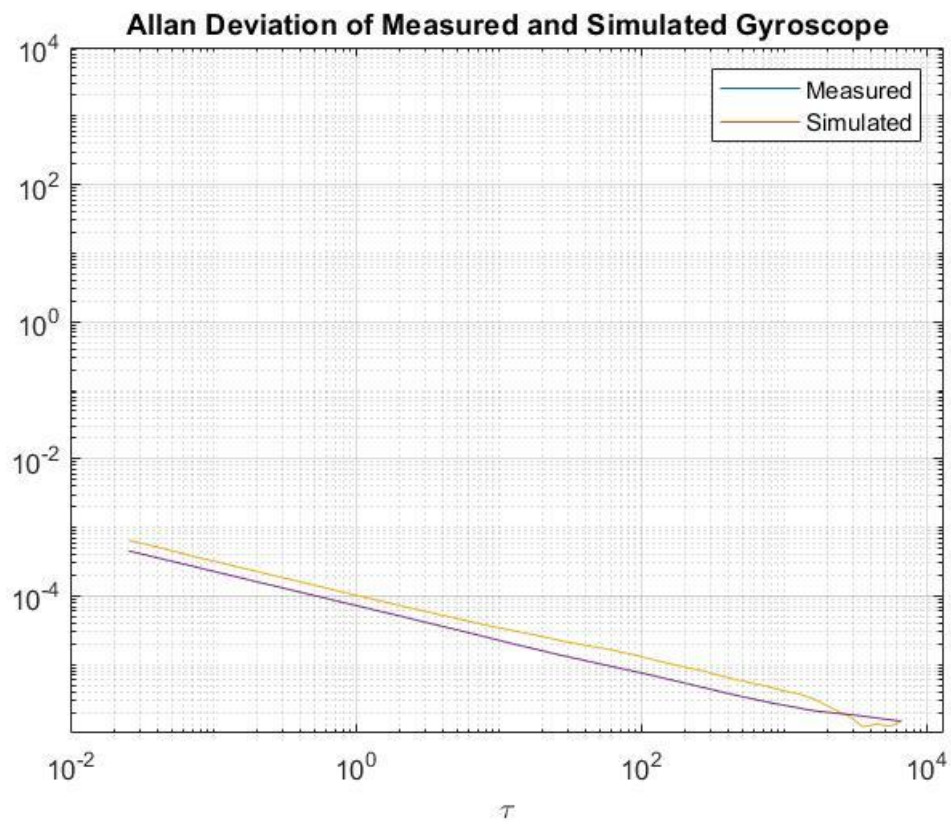
Errors in sensors could come from multiple sources - mechanical noise, electronic noise, environmental noise, and random noise; however, these errors could be broadly categorized as systematic and unsystematic. Systematic errors have similar or proportional values for every measurement, while unsystematic errors are random and vary unpredictably from one measurement to another. In an inertial sensor, both systematic and unsystematic errors contribute to output errors. Sources of systematic errors could be due to temperature effects, axis orthogonality, scale factor error, etc. In the Accelerometer and Gyroscope dataset for evaluating error distribution, the system is dominated by random errors which follow Gaussian distribution. However, magnetometer data is not following the gaussian distribution as closely as the Accelerometer and Gyroscope, which might be due to dominating systematic errors (soft and hard iron biases) in the environment. In a controlled environment, frequency distribution for magnetometers should also follow Gaussian Distribution.

VN-100 IMU uses AHRS Kalman Filter for estimating orientation data utilizing a fusion of Gyroscope, Accelerometer, and Magnetometer Data. Kalman Filter output is a weighted sum of the predicted state and measured state, so starting with initial measurement, the predicted state is always assumed to be more than the previous state (or moving), which gives an increasing trend with decreasing slope (as the system stabilizes) in the time-series plot for estimated values. Further, it is verified by the time-series plots for orientation data (Plot 8, Graph 1), which shows an increasing trend that stabilizes with time. Also, based on this inference, the frequency distribution plot for the orientation should not follow Gaussian Distribution as it is applicable for random noises, which is further verified by the Frequency distribution plot for Orientation data (Plot 8, Graph 2).

PLOTS

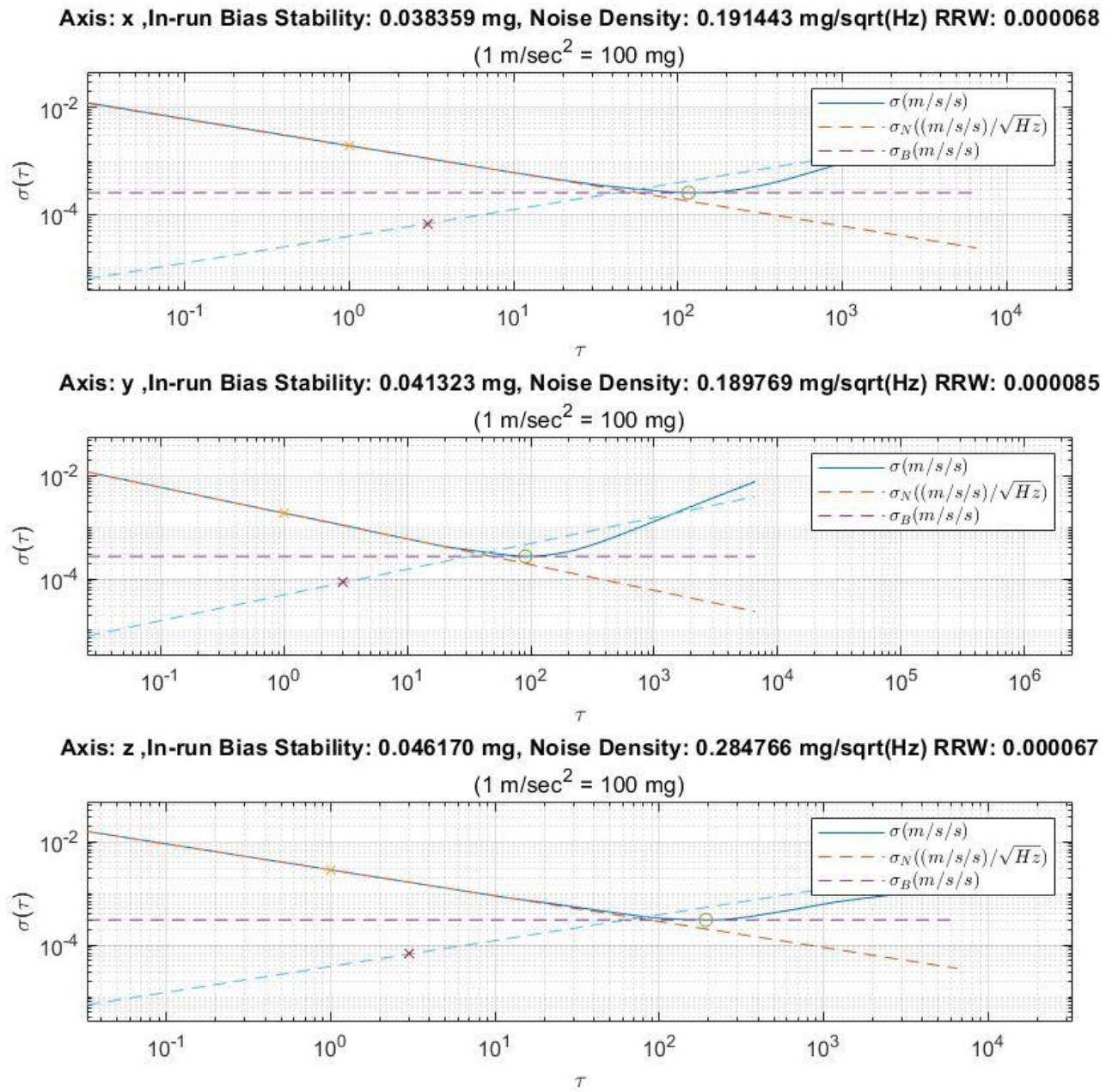


Plot1: Allan Deviation for Y-Axis in Gyroscope



Plot2: Simulated and Measured Allan Deviation for Gyroscope

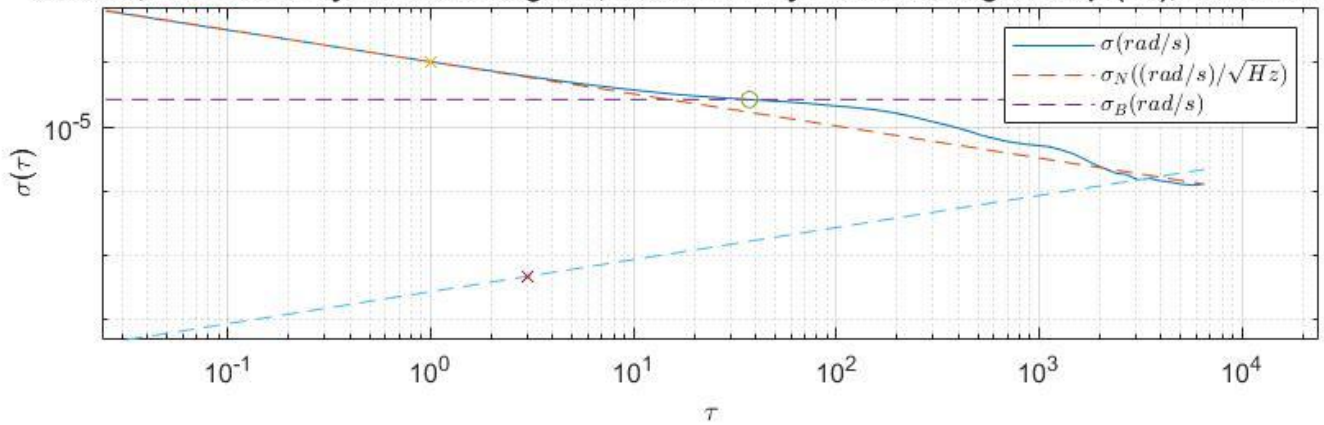
Accelerometer-Allan Deviation with Angle Random Walk and Bias Instability



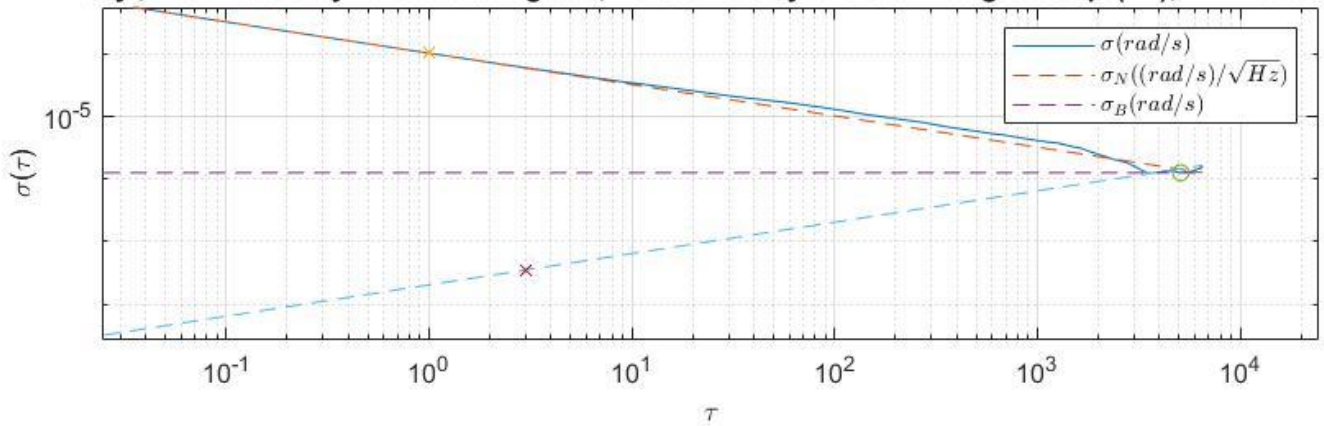
Plot 3: Allan Deviation in Accelerometer

Gyroscope-Allan Deviation with Angle Random Walk and Bias Instability

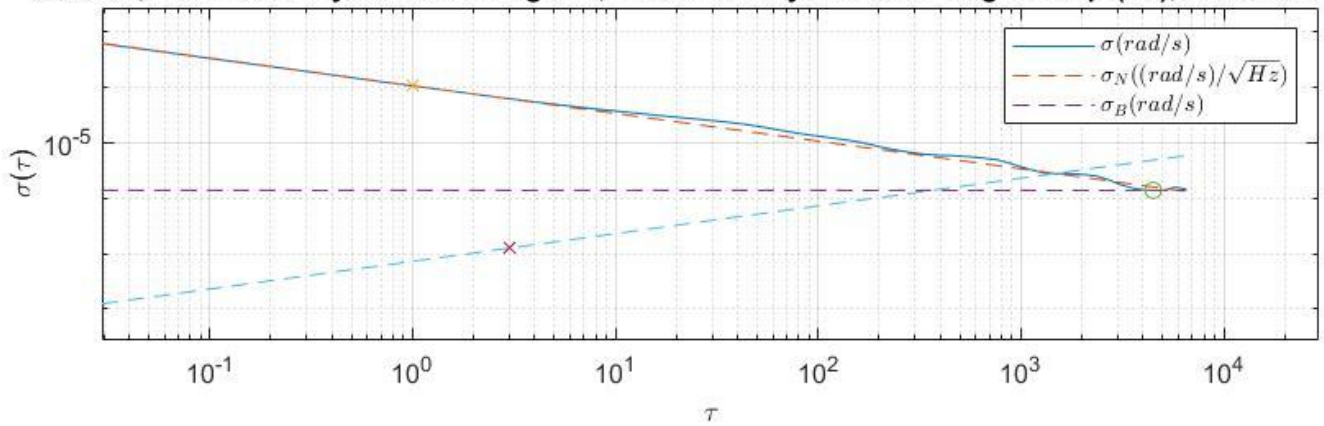
Axis: x ,Bias Instability: 0.002309 deg/sec, Noise Density: 0.005945 deg/sec/sqrt(Hz), RRW:0.000003



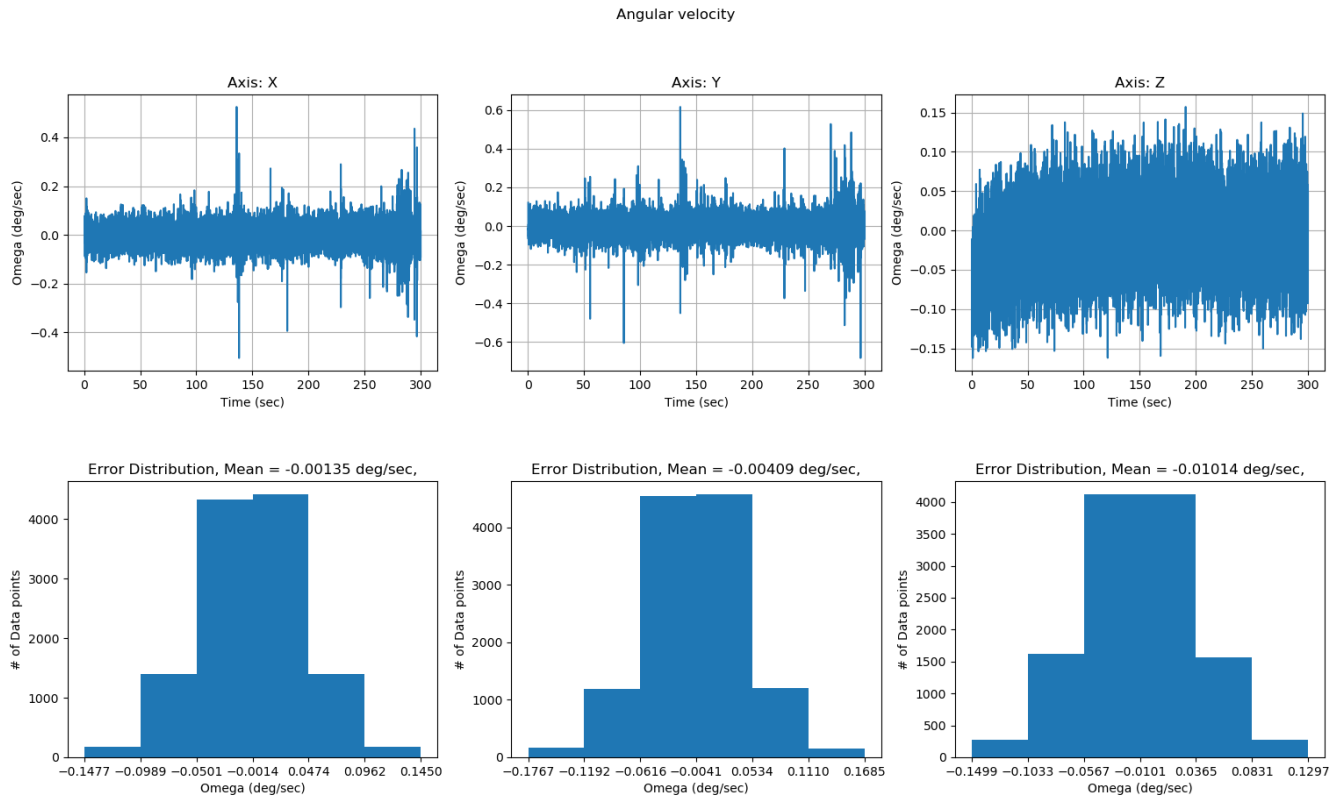
Axis: y ,Bias Instability: 0.000108 deg/sec, Noise Density: 0.005824 deg/sec/sqrt(Hz), RRW:0.000002



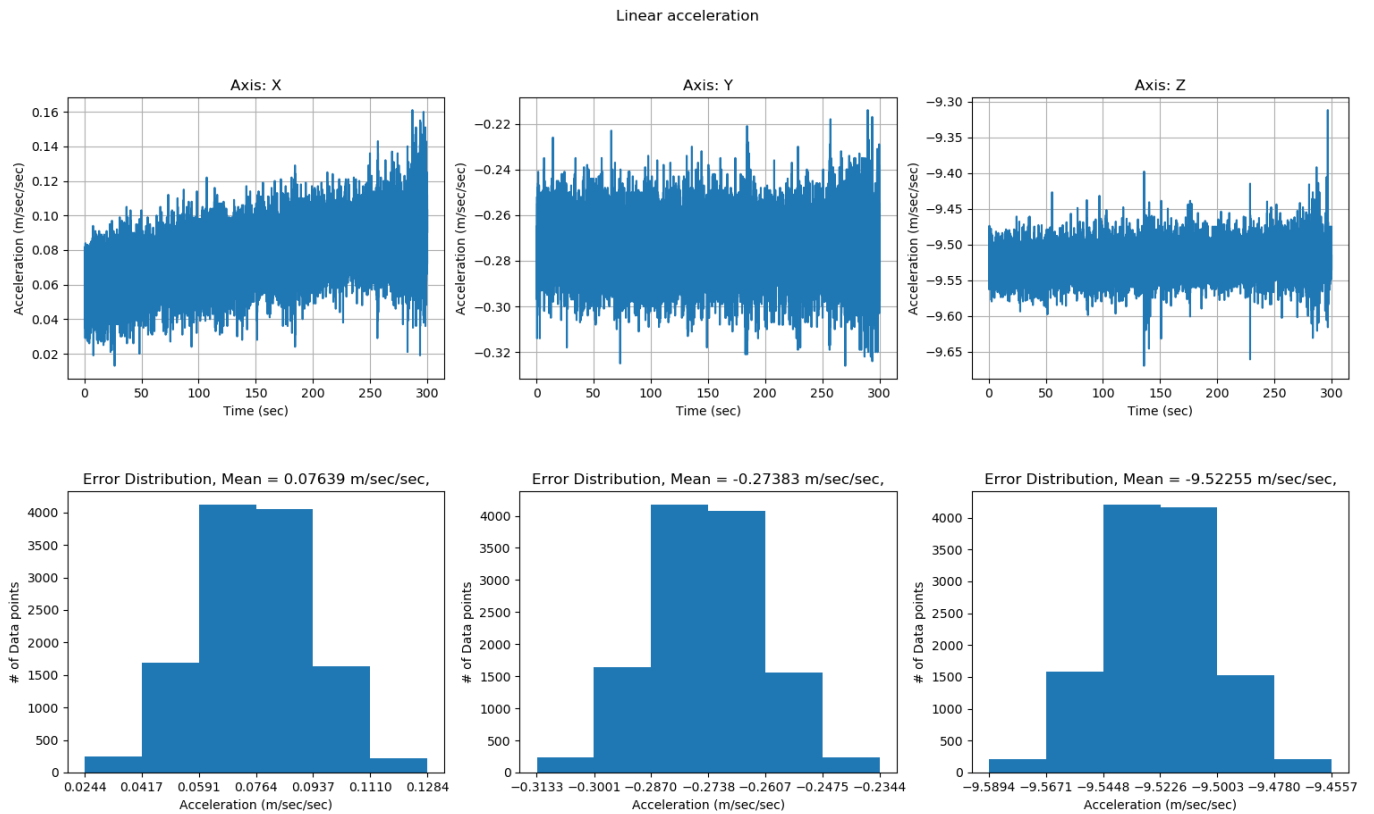
Axis: z ,Bias Instability: 0.000120 deg/sec, Noise Density: 0.006157 deg/sec/sqrt(Hz), RRW:0.000007



Plot 4: Allan Deviation in Gyroscope

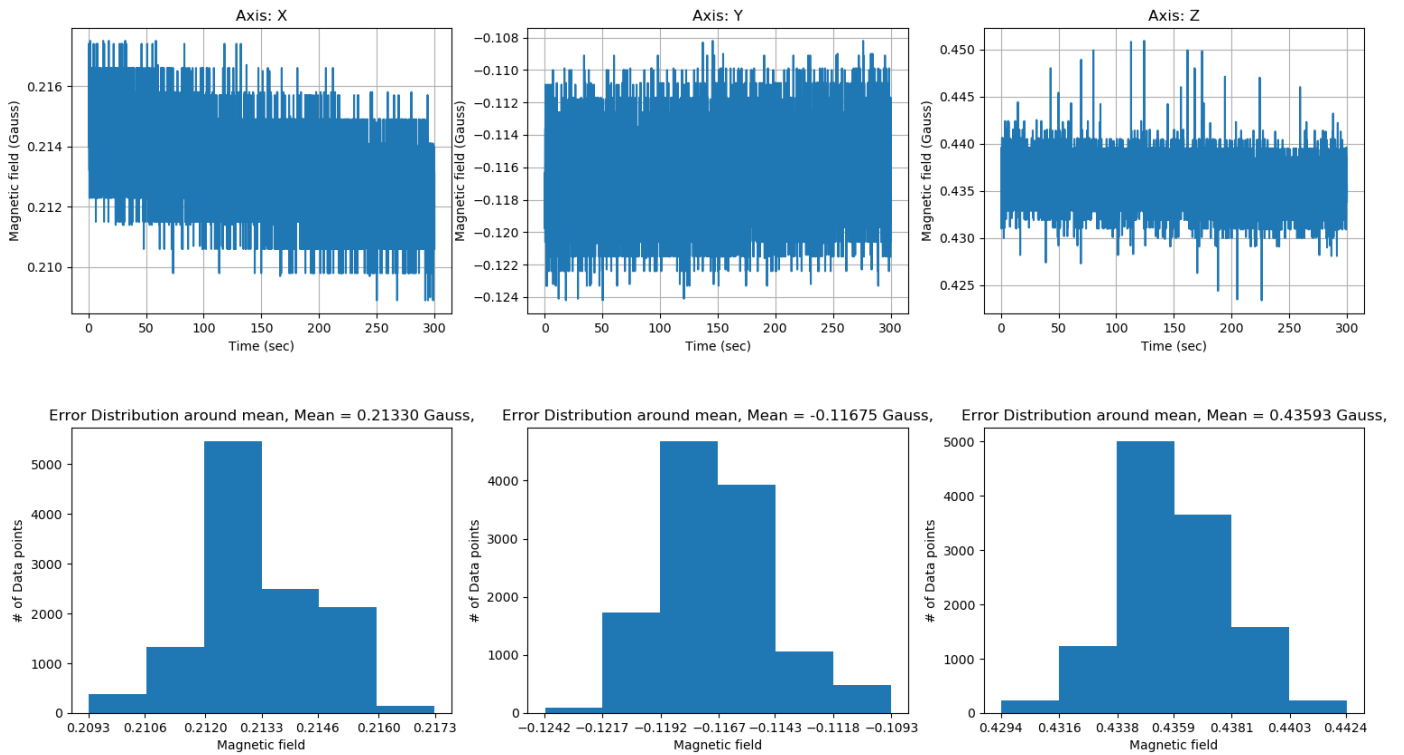


Plot 5: Time series and Frequency distribution for angular velocity



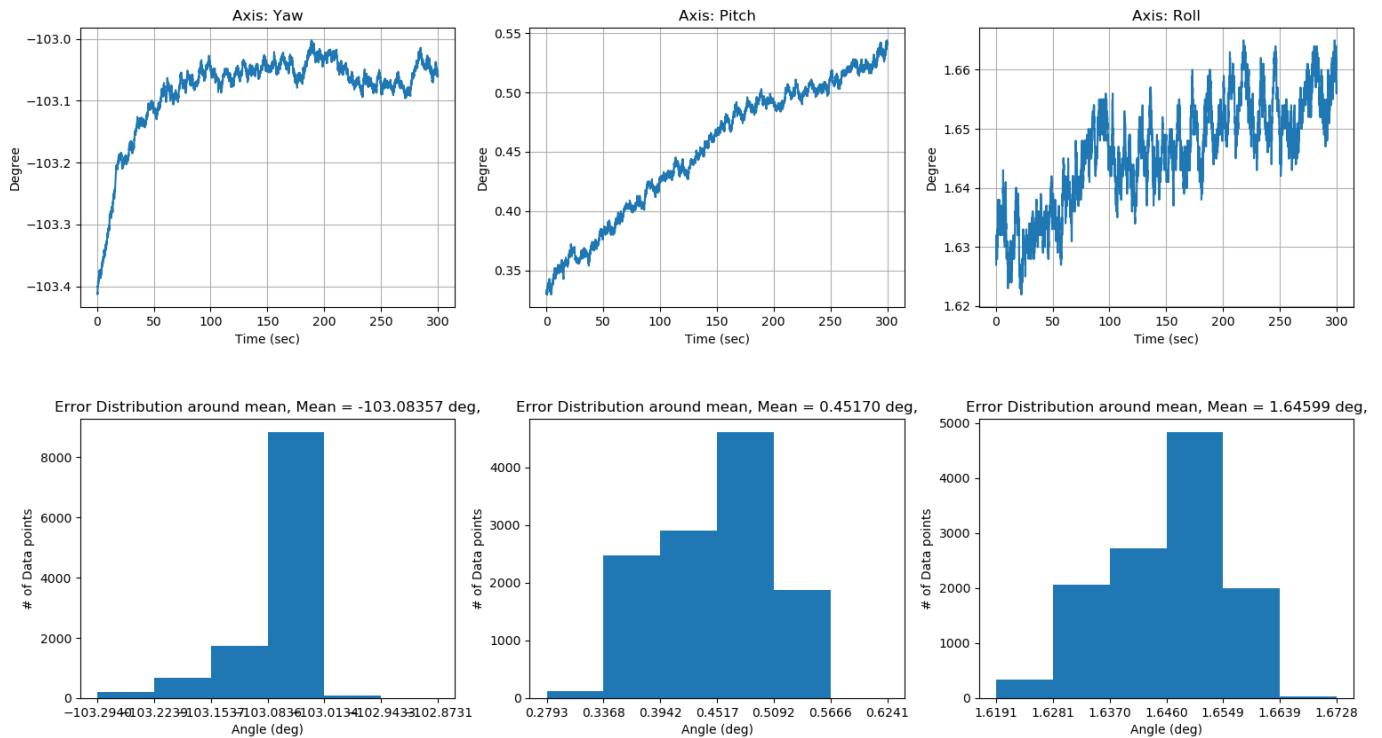
Plot 6: Time series and Frequency distribution for Linear acceleration

Magnetic field



Plot 7: Time series and Frequency distribution for Magnetic field

Orientation - Euler Angles



Plot 8: Time series and Frequency distribution for Orientation (Euler Angles: Yaw (z), Pitch (y), Roll (x))

References:

1. El-Sheimy, Naser & Hou, Haiying & Niu, Xiaoji. (2008). Analysis and Modeling of Inertial Sensors Using Allan Variance. *Instrumentation and Measurement, IEEE Transactions on*. 57. 140 - 149. 10.1109/TIM.2007.908635.
2. Farrell, J. A, Silva, F. O, Rahman, F., & Wendel, J. (2021). IMU Error Modeling Tutorial: INS state estimation with real-time sensor calibration. *UC Riverside: Bourns College of Engineering*. Retrieved from <https://escholarship.org/uc/item/1vf7j52p>
3. Allan variance Source: <http://en.wikipedia.org/w/index.php?oldid=580579047>
4. "IEEE Standard for Specifying and Testing Single-Axis Interferometric Fiber Optic Gyros," in IEEE Std 952-2020 (Revision of IEEE Std 952-1997) , vol., no., pp.1-93, 12 Feb. 2021, doi: 10.1109/IEEESTD.2021.9353434.
5. Törnqvist, David. "Statistical Fault Detection with Applications to IMU Disturbances." (2006).
6. Farahan SB, Machado JJM, de Almeida FG, Tavares JMRS. 9-DOF IMU-Based Attitude and Heading Estimation Using an Extended Kalman Filter with Bias Consideration. *Sensors*. 2022; 22(9):3416. <https://doi.org/10.3390/s22093416>
7. <https://github.com/ethz-asl/kalibr/wiki/IMU-Noise-Model>
8. [https://eng.libretexts.org/Bookshelves/Industrial_and_Systems_Engineering/Book%3A_Chemical_Process_Dynamics_and_Controls_\(Woolf\)/02%3A_Modeling_Basics/2.05%3A_Noise_modeling-_more_detailed_information_on_noise_modeling-_white%2C_pink%2C_and_brown_noise%2C_pops_and_crackles](https://eng.libretexts.org/Bookshelves/Industrial_and_Systems_Engineering/Book%3A_Chemical_Process_Dynamics_and_Controls_(Woolf)/02%3A_Modeling_Basics/2.05%3A_Noise_modeling-_more_detailed_information_on_noise_modeling-_white%2C_pink%2C_and_brown_noise%2C_pops_and_crackles)